Threatened species of Western Australia. (2004). (provided scientific information and photographic imagery)

Tracks Magazine of the Western Australian Museum. (2004). Esperance marine life under the microscope (provided photographic imagery)

Helix magazine. (2005). article and educational poster (provided scientific information and photographic imagery)

Reports

Kendrick, G.K., Harvey, E.S., McDonald. J.I., *et al.*, (2004). *Characterising the fish habitats of the Recherche Archipelago: Final Research Report*. Report to Fisheries Research and Development Committee

McDonald. J.I., and Fromont, J. (2004). *Sponge and ascidian communities of the Recherche Archipelago 3.* Report to CSIRO Strategic Research Fund for the Marine Environment

McDonald. J.I., and Fromont, J. (2004). *Sponge and ascidian communities of the Recherche Archipelago 2.* Report to CSIRO Strategic Research Fund for the Marine Environment

McDonald. J.I., and Fromont, J. (2003). *Sponge and ascidian communities of the Recherche Archipelago 1.* Report to CSIRO Strategic Research Fund for the Marine Environment

3.3.3 Understanding the natural variability of currents along the Western Australian coastline: Inter-annual variability of the Leeuwin Current

Investigators / Institutions

Alexis Berthot and Prof. Charitha Pattiaratchi	School of Environmental Systems Engineering, the University of Western Australia
Dr Ming Feng and Dr Gary Meyers	CSIRO Marine and Atmospheric Research
Dr Yun Li	CSIRO Mathematical and Information Sciences

Executive Summary

The Leeuwin Current is a warm, lower salinity, poleward flowing current, which flows along the continental shelf break of Western Australia and plays an important role in the region's marine environment and climate. The Current is driven by an alongshore steric height gradient, due to the meridional ocean cooling and the inter-connection between the Indian and Pacific oceans through the Indonesian Throughflow. In this study, the Simple Ocean Data Assimilation (SODA 1.4.2) reanalysis data for the 44-year period from 1958 to 2001 were used to determine the latitudinal variability of the Leeuwin Current along the coast of Western Australia in response to inter-annual variability. Results showed the alongshore slope was generally stronger (i.e. steeper slope) during La Niña years and weaker during El Niño years. The slope presented a positive (negative) linear trend during the PDO cool phase (warm phase). Composite maps also suggested the effect of ENSO was manifested in the simulated Leeuwin Current in the May–July period preceding the peak of ENSO in the Pacific Ocean and the response decays at higher latitudes.

Introduction

The Leeuwin Current System consists of three major currents: the southward flowing Leeuwin Current (LC) at the surface; the northward flowing Leeuwin Undercurrent (LU) at the sub-surface; and the northward flowing Capes and Ningaloo Currents on the continental shelf during summer. Generally, there is downwelling along the coast and local coastal upwelling due to equatorward wind and associated coastal currents during the summer. The Leeuwin Current is a warmer, lower salinity current, which flows poleward along the continental shelf break against the prevailing southerly winds (Thompson 1984; Godfrey and Ridgway 1985; McCreary et al. 1986; Batteen and Rutherford 1990; Godfrey and Weaver 1991; Smith et al. 1991; Clarke et al.1994; Meyers et al. 1995; Pearce and Pattiaratchi 1999; Feng et al. 2003). It is generated by an alongshore steric height gradient due to the poleward sea surface cooling (Thompson 1984; McCreary et al. 1986) and the presence of warm waters near the North West Shelf (NWS) (owing to the inter-connection between the Indian and Pacific oceans through the Indonesian Throughflow, Godfrey and Weaver 1991). Warmer, lower salinity water flows through the Indonesian archipelago from the Pacific to the Indian Ocean. This results in lower density water being present between Australia and Indonesia, when compared with the cooler and more saline ocean waters off south-western Australia. This density difference produces a change in sea level, of about 0.5 m, along the WA coast. Interaction of the Leeuwin Current with changes in the bathymetry and offshore water of different density results in the generation of eddies transported offshore, in particular, off Shark Bay, Abrolhos Islands, Jurien Bay, Rottnest Island and Cape Leeuwin (Andrews 1977; Cresswell and Golding 1979; Pearce and Griffiths 1991; Batteen et al. 1992; Batteen and Butler 1998;, Feng et al. 2005).

The Leeuwin Current has seasonal and inter-annual variability: it is globally stronger, during winter and under La Niña conditions and weaker during summer and El Niño conditions (Smith et al. 1991; Feng et al. 2005). However, the Leeuwin Current System's inter-annual variability is not completely understood. The recently developed reanalysis ocean climate data provides an ideal tool to investigate the Leeuwin Current decadal and multidecadal variations. The Simple Ocean Data Assimilation (SODA 1.4.2) reanalysis of ocean climate for the 44-year period from 1958 to 2001 (Carton and Giese, 2005), was used to determine the latitudinal variability of the Leeuwin Current along the coast of Western Australia in response to inter-annual variability.

Aims and Objectives

This project aimed to quantify the natural variability of the oceanic circulation off Western Australia through the analysis of long-term data sets. Study results are directly relevant to managers charged with establishing a network of marine protected areas, management of fish stocks and environmental protection as well as other researchers in the marine environment handling field data and studying the physical and ecological systems. Knowledge of the physical environment's natural variability (in most cases, this variability is responsible for the pelagic and benthic ecological responses) is crucial for management.

This project's objectives are to develop:

- an enhanced understanding of the natural variability of the nearshore and continental shelf current systems off Western Australia
- advanced statistical methods to detect climate change signals
- regional climate change scenarios for circulation off Western Australia
- the results presented in this paper are addressing the first point

Data Sources

Simple Ocean Data Assimilation (SODA) reanalysis data, version 1.4.2 (Carton and Giese, 2005) was used in this study. The re-analysis covered the 44-year period from 1958 to 2001;

and was spanned by daily surface winds from the European Center for Medium Range Forecasts ERA-40 atmospheric reanalysis. The reanalysis used direct observations in order to improve the ocean simulations. Carton and Giese (2005) provided details of the SODA reanalysis and the assimilation methods used. The reanalysis is available in a monthly-averaged form on a 0.5° x0.5° horizontal resolution and 40 vertical levels, gradually increasing from a 10 m-layer thickness to 250 m for the deepest layer. In this study, only the first 300 m of the ocean were considered and an interpolation into a constant 10 m-layer-thickness grid was undertaken. The period from 1960 to 1990 was used to calculate the variable anomalies extracted from the SODA 1.4.2 reanalysis.

Carton and Giese (2005) showed that, to the north of Australia, the reanalysis of the warm water exchanges between the Pacific and Indian oceans through the Indonesian archipelago was similar to the observed estimates. When the seasonal cycle was removed, Carton and Giese (2005) indicated that the monthly reanalysis sea level and TOPEX/Poseidon altimetry were correlated in excess of r = 0.7. Additionally, in the present study, the SODA 1.4.2 reanalysis data were compared with real observations to demonstrate the data's validity for the investigation of the Leeuwin Current System's variability.

The transport calculated from SODA reanalysis was generally within an average of +/–12% accuracy with the transport Feng et al. (2003) and Meyers et al. (1995) calculated from their observations. The SODA Sea Surface Height (SSH) anomaly was compared with the Fremantle Sea Level anomaly. The SODA SSH anomaly standard deviation of 51.78 mm was smaller than the Fremantle sea level anomaly standard deviation of 70.31 mm; nevertheless, the datasets were correlated at 0.7.

SODA reanalysis temperature data were also compared with an eXpendable BathyThermograph (XBT) transect starting from Fremantle and extending north-westward as far as 100°E (Wijffels and Meyers, 2004). The correlation between the XBT temperature data and the interpolated reanalysis data for the same period (1983–-1999) was generally high and up to 0.8 in the first 100 m below the surface and near the coast; from 100 to 400 m, correlation was only about 0.4–0.5. However, there was generally a strong correlation between the two datasets in the area that comprised the Leeuwin Current, which is the focus of this study.

ENSO years

In this study, the ENSO events that occurred from 1958 to 2001, the period of the SODA reanalysis data set, were isolated by considering the monthly SOI and monthly Niño3 for El Niño years and monthly SOI and monthly Niño3.4 for La Niña years (Table 3.2). El Niño years are defined when six consecutive months of Niño3 three-month average are above 0.5 units of standard deviation (STD) and four consecutive months of the three-month average SOI are below 0.5 STD.

Table 3.2. El Niño and La Niña years. : El Niño years are based on the monthly SOI and monthly Niño3, and La Niña years are based on the monthly SOI and monthly Niño 3.4.

El Niño	1963, 1965, 1969, 1972, 1982, 1976, 1987, 1991, 1997
La Niña	1964, 1970, 1971, 1973, 1974, 1975, 1988, 1989, 1998, 1999, 2000

Results

Eddy kinetic energy

The presence of mesoscale eddies have been identified on the Leeuwin Current's western side (Andrews 1977, Cresswell and Golding 1979; Pearce and Griffiths 1991). Batteen et al. (1992) showed the generation of these eddies resulted from a mixed barotropic and baroclinic instability and that eddies have timescales of months and grow on scales around 150 km. The current's offshoots and meanders tend to occur at preferred locations along the coast, such as: Shark Bay,

Abrolhos Islands, Jurien Bay, Rottnest Island, and Cape Leeuwin. The highest values of Eddy Kinetic Energy (EKE) are found off Western Australia south of 30°S (Batteen and Butler 1998) and between 30°S and 32°S (Feng et al. 2005). Eddy energy is weak during austral summer and El Niño years and strong during austral winter, and La Niña years (Feng et al., 2005).

The eddy kinetic energy was calculated here using the SODA surface current velocities. The mean EKE over 1958–2001 had a maximum of 180 $cm^2\ s^{-2}$ situated at 28.75°S (Figure 3.17a). The location of the maximum was lower in latitude compared with the results from Feng et al. (2005); this could be due to the coarse SODA reanalysis grid and limited coastline resolution. On an annual cycle, the mean EKE maximum moved southward from summer to the following spring (Figure 3.17b), more precisely, it was located at 27°S in summer, 28°S in fall, 30°S in winter, and 32°S in early spring. The strongest eddies were generated at lower latitudes during summer; as the current strength increased from north to south and from the end of summer to its maximum in winter, eddies were gradually generated at higher latitudes.

Sea surface height slope and ENSO

The general consensus is that the Leeuwin Current's driving force is an alongshore steric height gradient, which overwhelms the opposing equatorward wind stress (Thompson et al. 1984; Godfrey and Ridgway 1985; McCreary et al. 1986). Godfrey and Ridgway (1985) suggested the high surface dynamic height field present north of Western Australia (set by the flow of low-density Pacific Ocean water into the Indian Ocean trough the Indonesian Throughflow) might remotely force the Leeuwin Current. Although McCreary et al. (1985) showed that thermohaline forcing due to the poleward increase of surface density in the ocean interior might be considered as the main forcing of the Leeuwin Current, they concluded that the remote forcing mechanism proposed by Godfrey and Ridgway (1985) may also contribute to the Leeuwin Current.

Although Leeuwin Current forcing may be a combination of several mechanisms, an interesting way of quantifying this forcing is to determine the slope along the WA coast. A transect along the location of the maximum southward transport, i.e. Leeuwin Current, is considered (Figure 3.18a). The slope anomaly was determined to isolate periods of steep and weak slope (Figure 3.18b). On the annual scale, the slope was steeper in winter and weaker in summer. Early in the year it exhibited a strong dependence on that of the previous year; thus the May-to-December average slope anomaly (bars) was considered here to represent the characteristics of a particular year and to determine the slope's interannual variability.

The May-to-December average slope anomaly is generally negative during El Niño (weaker slope) and positive during La Niña (i.e. steeper slope). Few El Niño years (i.e. 1972, 1991) presented a slightly positive slope anomaly, and few La Niña years (i.e. 1975, 1988, 1989) presented a slightly negative slope anomaly. However, the averaged sea surface height along the transect (Figure 3.18b) appeared significantly low during these particular El Niño years and high during these La Niña years. This was consistent with Feng et al.'s (2003, 2004) study showing the Fremantle sea level had a strong linear dependence with ENSO and could be used as an index for the Leeuwin Current's strength on annual and interannual timescales.

Overall, Leeuwin Current' forcing was responding to ENSO and appears to be weaker during El Niño and stronger during La Niña.

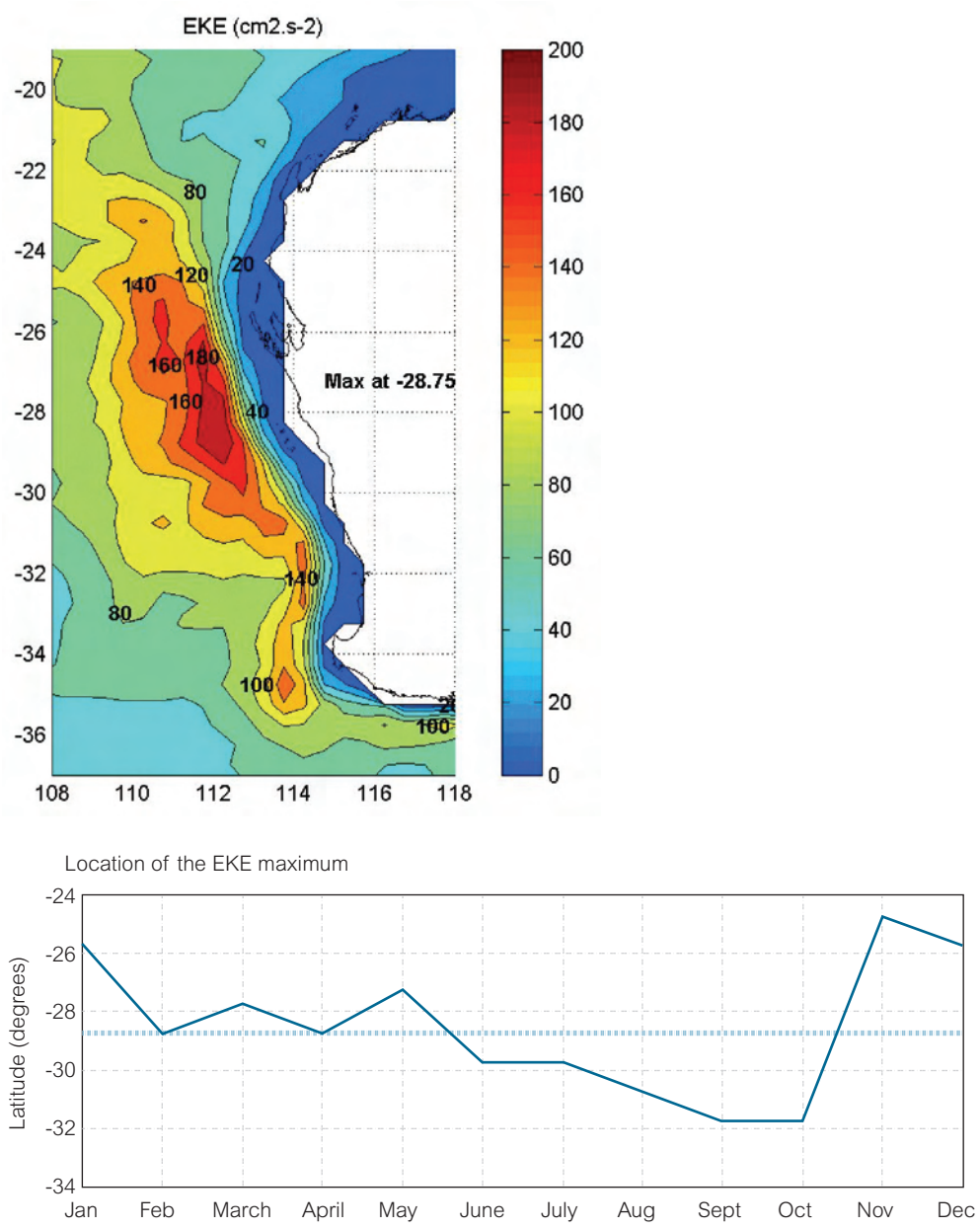

Figure 3.17: Eddy Kinetic Energy (EKE). a) mean EKE (in $cm^2\ s^{-2}$); and b) location of the monthly mean EKE maximum over 1958–2001 calculated from SODA reanalysis surface velocity current data. The yearly mean EKE maximum is situated at 28.75°S.

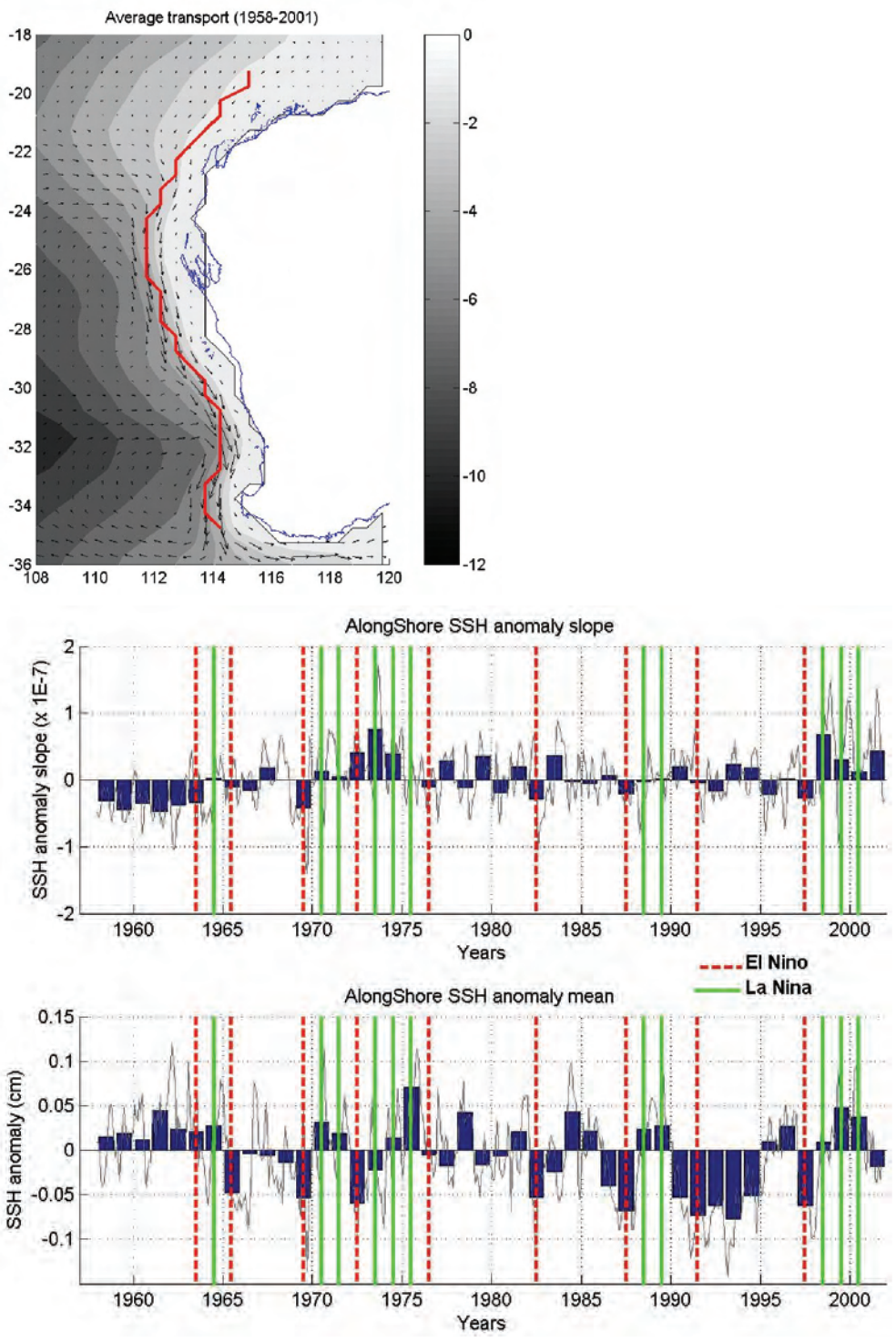

Figure 3.18: (a) Location of the maximum southward transport (red line). Arrows represent the 1958–2001 average transport, and contour plots represent the cumulated southward transport from the coast. (b) Sea surface height anomaly slope (top) and mean sea surface height anomaly (bottom), calculated along the location of the maximum southward transport (i.e. Leeuwin Current location). Bars represent the May-to-December average slope anomaly. Vertical, red, dashed lines (vertical, green line) represent El Niño (La Niña) years.

Sea surface height slope and Pacific Decadal Oscillation (PDO)

The Pacific Decadal Oscillation (PDO) is a long-term ocean fluctuation of the Pacific Ocean (Mantua et al. 1997; Zhang et al. 1997). A cool wedge of anomalously low sea-surface heights/ocean temperatures in the eastern equatorial Pacific and a warm pattern of higher than normal sea-surface heights connecting the north, west, and southern Pacific characterise the PDO cool phase. In the PDO warm phase, the west Pacific Ocean becomes cool and the wedge in the east warms. The SODA reanalysis data (1958–2001) covered two PDO cool phases 1960–1976 and 1998–200 and one PDO warm phase from 1977–1997.

The SSH anomaly slope along the Leeuwin Current presented a positive linear trend during the PDO cool phase and a weakly negative linear trend during the PDO warm phase (Figure 3.19). The SSH anomaly over the western Pacific (0–10°N 130–150°E box) showed a similar trend. During a PDO cool phase, a warm water/high sea surface height accumulation may develop in the Indonesian archipelago; the reverse (i.e. lower sea surface height) occurs during the PDO warm phase. During a PDO cool phase, the long-term accumulation of high sea surface height/ocean temperature in the western Pacific may be transmitted to the Indian Ocean, and more particularly to the north-west Western Australia, via the Indonesian Throughflow (Clarke and Liu 1994). Thus the slope in the sea surface height extending from the north-west to the south-west of Western Australia may increase. The reverse is expected during a PDO warm phase. The Leeuwin Current forcing therefore increases (decreases) during a PDO cool phase (warm phase).

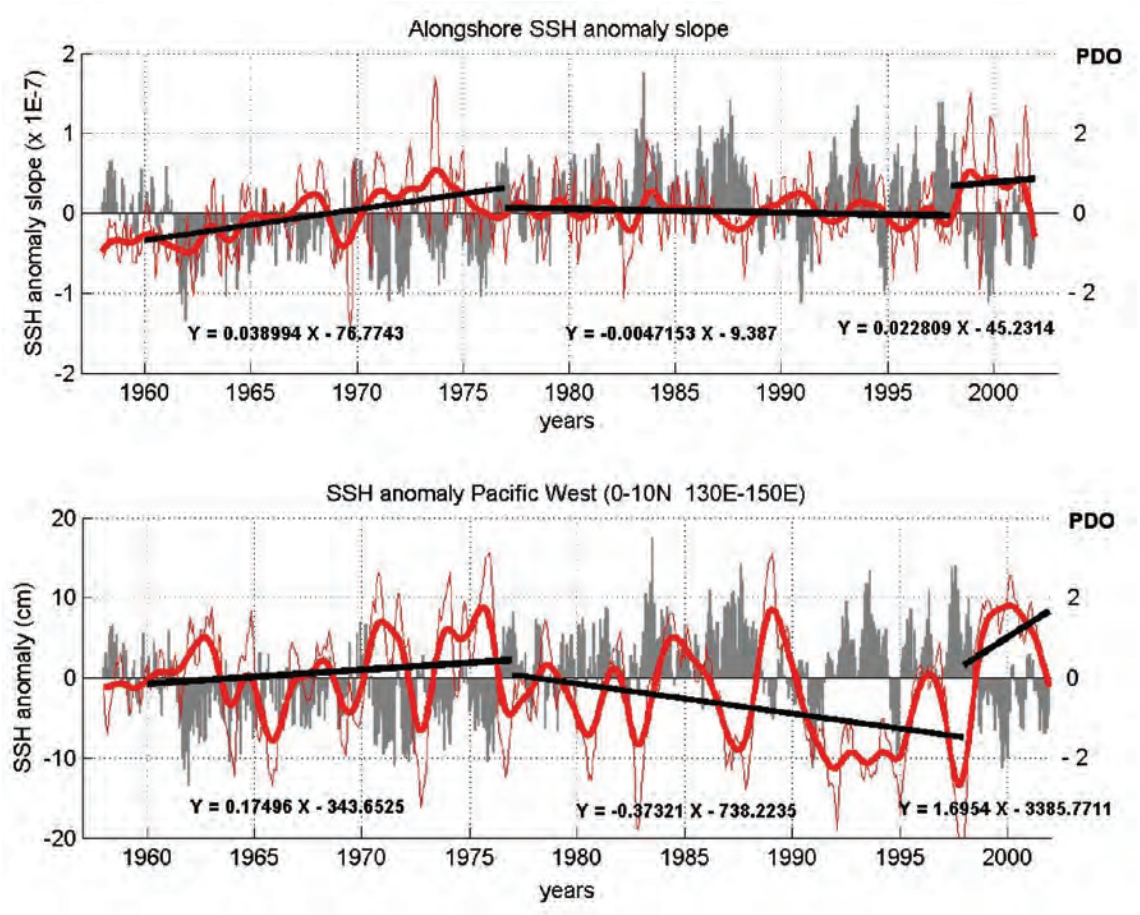

Figure 3.19: Pacific Decadal Oscillation (grey bars) and sea surface height slope anomaly (red line). The thick, red line represents the SSH anomalies filtered with a 19-year Hanning filter. Black lines represent positive (negative) linear trends during PDO cool (warm) phases.

Transport variability and ENSO

The Leeuwin Current flows southward along the continental shelf of Western Australia. Seven transects were extracted to determine the interannual variability's net transport along the coast (Figure 3.20). They extend to five degrees of longitude offshore (i.e. ~500 km) from the coast. Sensitivity tests were undertaken by considering transects of +/– 0.5 degrees of longitude (i.e. +/– 10% in length). Sensitivity of the transport calculation to the transect length was not considered significant at 95% confidence.

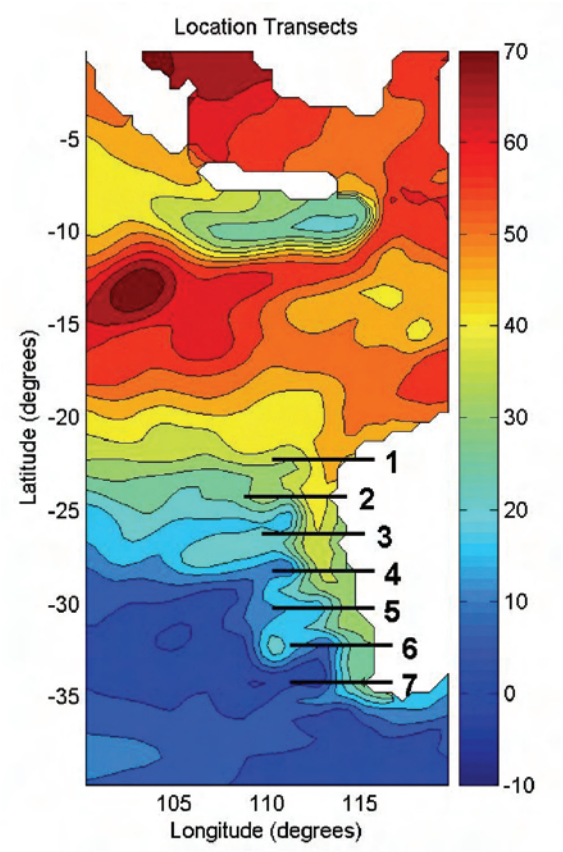

Figure 3.20: Location of the seven transects along the Western Australian coastline. Contours represent the mean sea surface height in cm (from SODA reanalysis) over 1958 to 2001.

From 24°S to 34°S, the mean net transport was southward of 3–4 Sv. Farther north at 22°S, the mean net transport was only 1.7 Sv southward. The weak southward transport at lower latitudes was due to the weak offshore geostrophic present at this latitude and also to the presence of the Ningaloo Current flowing northward near the coast during summer. Examination of the transport across all transects showed that a strong, yearly southward transport at lower latitudes might not remain as strong compared with the other years at higher latitudes, and vice versa. A measure of the Leeuwin Current transport at a particular point along the coast does not necessarily provide insight into the Leeuwin Current's overall strength along the coast.

During El Niño years (la Niña years), sea surface temperature cooling (warming) occurs in the western tropical Pacific and Java Sea as early as the austral autumn preceding the peak of ENSO in the tropical Pacific Ocean (SST composites not shown here) (Van Loon H. 1972a, 1972b). ENSO is 'felt' by the Leeuwin Current as early as during the May-July preceding the peak of ENSO in the Pacific in December. The composites map of the southward transport during the end of autumn/beginning of winter demonstrates the accumulated southward transport from the coast is much larger in the north of Western Australia during La Niña years (Figure 3.21).

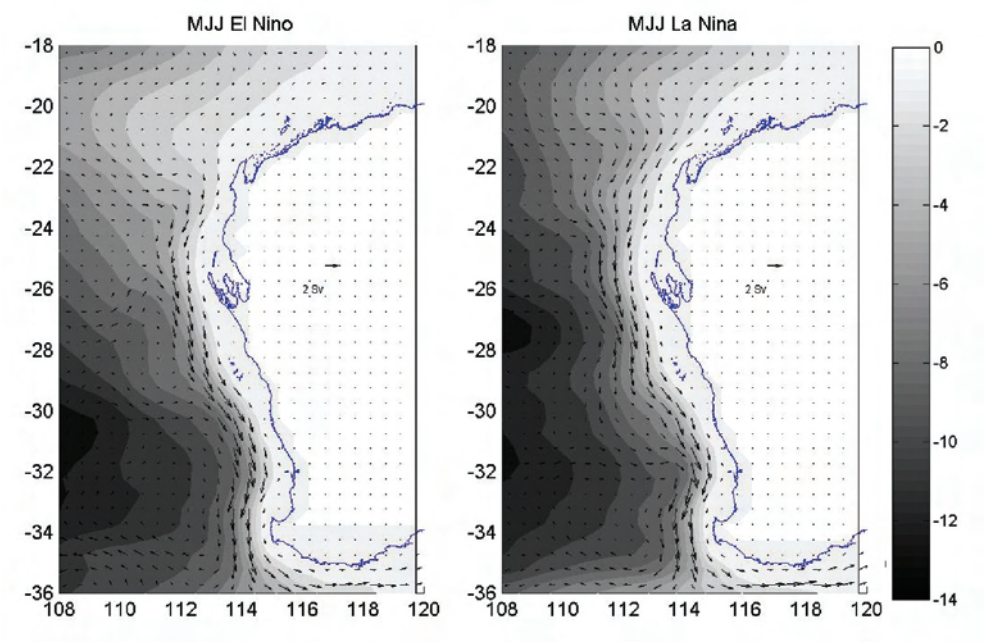

Figure 3.21: Composites map of the southward transport (Sv) during El Niño/La Niña events for May-June-July period.

The transport along the coast was further investigated by examining composites of the net transport across the seven transects presented in Figure 3.20. Generally, transects showed a maximum net southward transport near May–June and a minimum net southward transport in January–February as well as near September (Figure 3.22). As shown previously the location of the highest eddy kinetic energy (EKE) occurred offshore of the main current axis, around 28.75°S. The Leeuwin Current's response to ENSO appeared to be different between north and south of the EKE maximum.

Transects 1, 2, 3, and 4, situated north of the EKE maximum, presented a stronger net southward transport during most of the year for La Niña years than for El Niño years. Transects 5, 6, and 7, situated south of the EKE maximum, presented a net transport with different characteristics throughout the year. During autumn and winter, the net southward transport was equal or even weaker (transect 6), for La Niña years than for El Niño years. From the end of winter to summer the net southward transport was mostly stronger for la Niña years. In summer, when the Leeuwin Current was weak, no significant differences existed between El Niño and La Niña years.

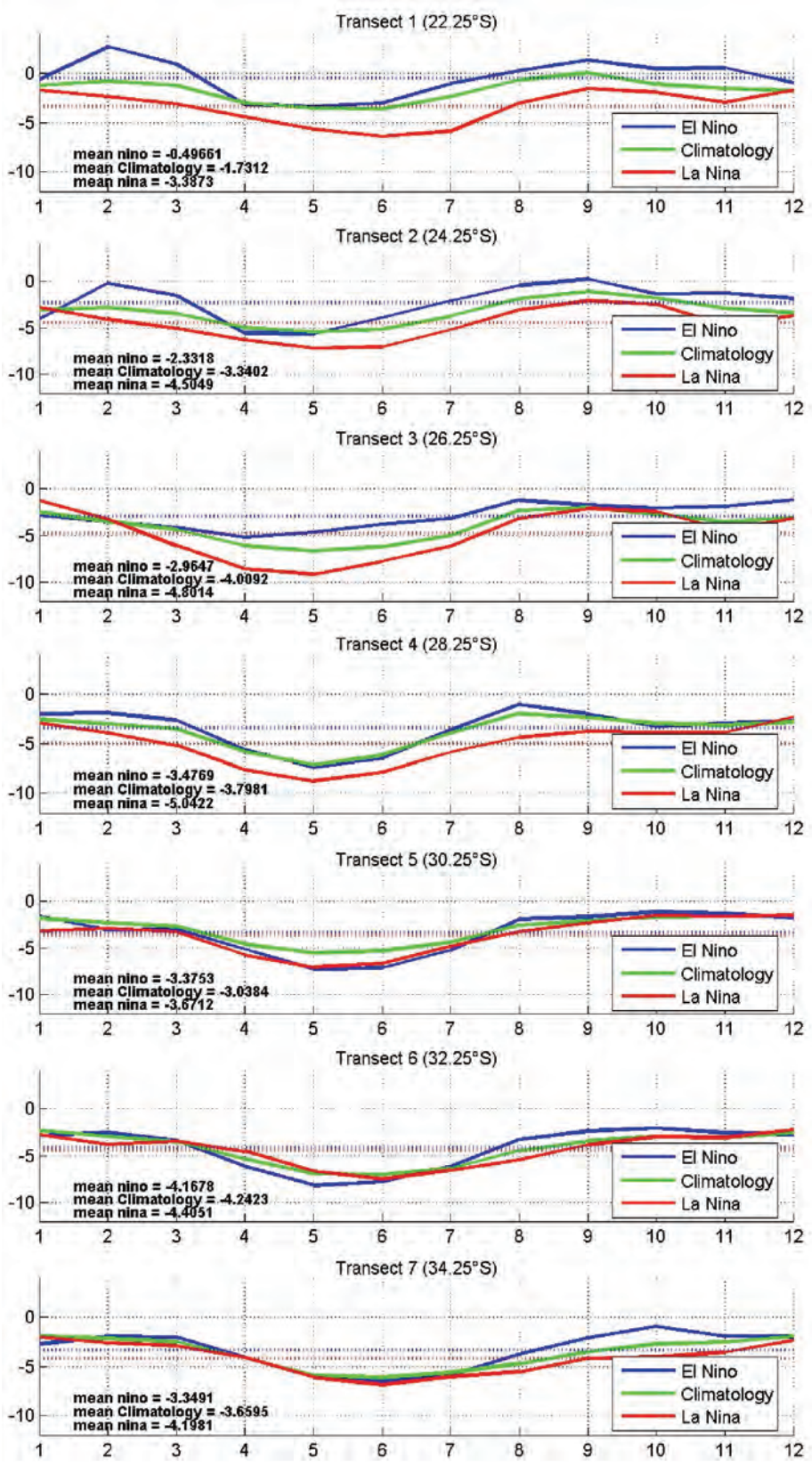

Figure 3.22: Yearly composites of the net transport (in Sv) across the seven transects along the coast of Western Australia, showing the transport variability throughout the year during El Niño and La Niña events. Negative values of transport indicate a southward transport.

Feng *et al.* (2003) showed, using XBT data, that the averaged geostrophic transport east of 110°E long 32°S was weaker all year around during El Niño years than during La Niña years. The net transport from 0-300m depth of the seven transects was calculated in two ways: first, using the SODA reanalysis velocity current; and second, by calculating the geostrophic current velocities relative to the 300 m level, using the SODA reanalysis temperature and salinity data, similar to Feng *et al.* (2003).

Only two transects are presented here (Figure 3.23a, b), one north (transect 2) and one south (transect 6) of the EKE maximum. The composite profiles were also averaged over three months. In the first 100 m depth, the transport calculated with the reanalysis velocities presented sharper variation, as the current was more variable over the continental shelf.

North of the EKE maximum (transect 2), the net transport and net geotrophic transport presented similar profiles across the depth, and the net transport during La Niña years was stronger than during El Niño years.

South of the EKE maximum (transect 6), the composites of net transport and net geostrophic transport presented similar characteristics during most of the year but not during the April–June period (i.e. transect 6, months month 4, -5, -6), the net transport calculated from actual current velocity was weaker during La Niña years than El Niño years across the whole depth, which is consistent with the results shown in Figure 3.22.

The 300 m-level is commonly used to determine the geostrophic current; it is considered the level of no motion and isolates the Leeuwin Current from the Leeuwin Undercurrent (LUC) present below this depth. However, it appeared that north of the EKE (transect 2), the net transport near the 300 m-level was weakly positive, indicating the northward flowing Leeuwin Undercurrent (i.e. positive net transport) was present between 200 and 300 m during most of the year, and was particularly strong at the end of winter (July–September) South of the EKE maximum (transect 6), the level of no motion appeared to be generally near 300 m-depth, indicating that the LUC was flowing northward below 300 m.

Discussion

Although a combination of a thermohaline forcing (McCreary et al. 1985) and remote forcing (due to interconnection between the Pacific Ocean water and the Indian Ocean) may drive the Leeuwin Current (Godfrey and Ridgway 1985), the sea surface height slope along the Leeuwin Current's maximum transport location may provide an effective quantification of this forcing and is a useful tool to describe its variability. From the results presented here, the forcing (i.e. sea surface height slope) generally appeared weaker during El Niño and stronger during La Niña. The sea surface height slope also presented a linear dependence with the different phases of the PDO. During a cool phase of the PDO, the slope increased linearly, due to the transfer of high sea surface height accumulated in the western Pacific. The reverse happened during a warm phase of PDO, with a decrease in the slope due to the transfer of low sea surface height. The Leeuwin Current forcing, represented here by the slope, responded to the PDO with similar dynamics than for ENSO, but on an inter-decadal scale.

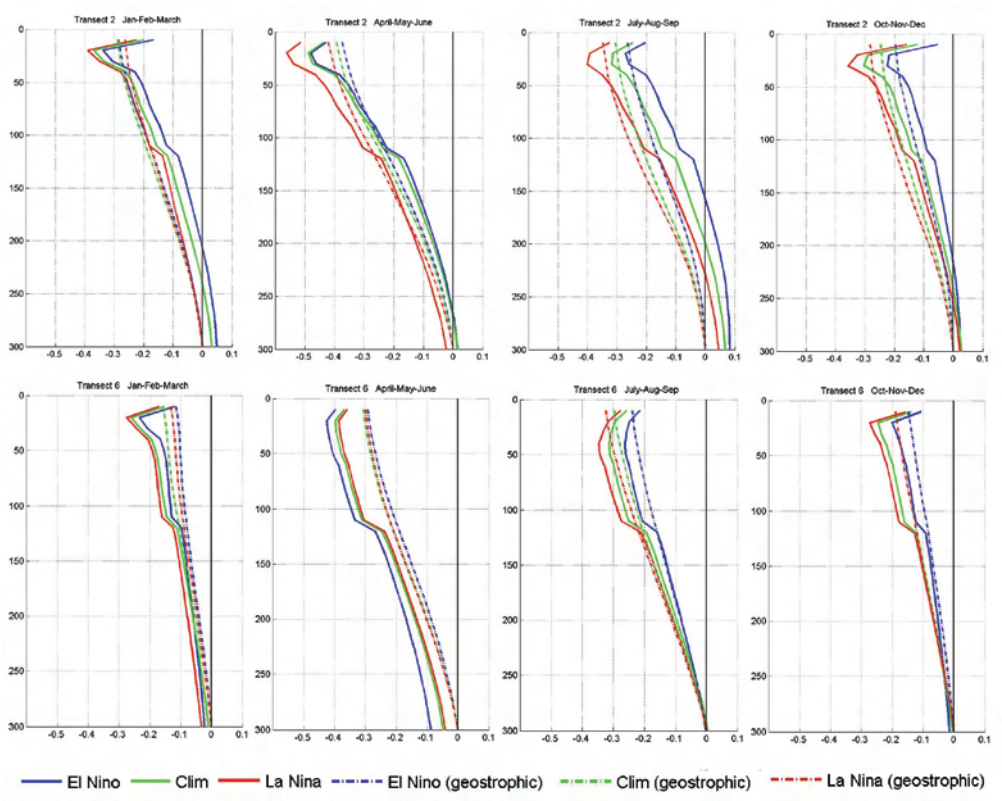

Figure 3.23: Composites profiles of the net transport (solid line) and net geostrophic transport (dashed line) across two transects along the coast of Western Australia, showing the average transport over three months during El Niño and La Niña years. Transport is in Sverdrup and negative values of transport indicate a southward transport.

Eddies develop on the offshore side of the Leeuwin Current core. As the eddies propagate westward, advection of warm water offshore, and thus energy, is drawn away from the mean current (Batteen and Butler 1998, Fang and Morrow 2003, Feng et al. 2005). The magnitude of these eddy fluxes has been estimated at 20–30% of the annual mean poleward heat and salt flux (Morrow et al. 2003). Eddies were generated at preferred locations, where the coastline significantly changed (Batteen and Butler 1998); nevertheless, an eddy kinetic energy maximum was located near 30°S (Batteen and Butler 1998, Feng et al. 2005) and near 29°S in the present study. Although it was demonstrated the EKE maximum location varied seasonally, most of the offshore advection of energy could have been occurring near 29–30°S.

Investigation of the transport along the Western Australian coastline showed the transport was very variable latitudinally. A measure of the Leeuwin Current transport at a particular point along the coast does not accurately provide insight into the Leeuwin Current's overall strength. The presence of eddies that draw energy from the Leeuwin Current into the Indian Ocean as well as the variability in the geostrophic input from the west into the Leeuwin Current may be responsible for the transport magnitude variability from the north to the south of Western Australia.

Composites of net transport along the coast showed the response to ENSO was variable between 22°S and 34°S. North of the EKE maximum, the Leeuwin Current's southward transport was stronger during La Niña years than during El Niño years. The southward transport at higher latitudes did not appear to respond to ENSO, and particularly from April to June when the Leeuwin current strength is maximum. The Leeuwin Current also appeared to be shallower at lower latitudes.

McCreary *et al*. (1986) suggested that a Leeuwin Current remotely forced by the flow of warm water from the Pacific Ocean into the Indian Ocean should weaken away from the forcing region, i.e. North West Shelf (NWS). Batteen and Butler (1998) showed that away from the source region, the influence of the NWS water diminished poleward, but was still strong enough to augment the onshore geostrophic inflow. This could partially explain the Leeuwin Current's weaker response to ENSO at higher latitudes. However, the thermohaline forcing, due to the poleward increase of surface density (McCreary 1986; Thompson 1984, Mc Creary 1986), should not be stronger during El Niño years; and therefore, the thermohaline forcing cannot be responsible for the stronger transport present at high latitudes during April–May-June of El Niño years.

Eddy energy is strong during La Niña years; more eddies are generated and more energy is advected offshore, away from the Leeuwin Current core. This may explain why the southward transport south of the maximum eddy generation was weakened. The Leeuwin Current is expected to be stronger at lower latitudes (north of 29–30°S) during La Niña years than during El Niño years. At higher latitudes, the influence of ENSO is not significant and the Leeuwin Current's strength may rely on other parameters.

Acknowledgements

This work is supported by the Strategic Research Fund for the Marine Environment (SRFME) a joint venture between the Western Australian State Government and the Commonwealth Scientific and Industrial Research Organisation (CSIRO).

REFERENCES

Andrews, J.C.., (1977). Eddy structure and the West Australian current. *Deep-Sea Research*, vol.*,* 24, pp. 1133–1148.

Batteen, M.L., J. Rutherford, M.J. (1990). Modeling studies of Eddies in the Leeuwin Current: The role of Thermal Forcing. *Journal of Physical Oceanography*, vol. 20, pp. 1484–1520.

Batteen, M.L., Rutherford, M.J., Bayler, E.J. (1992). A numerical study of wind- and thermal -forcing effects on the ocean circulation off Western Australia. *Journal of Physical Oceanography*, vol. 22, no. (12 pp.), 1406–1433.

Batteen, M.L. and Butler, C.L., (1998). Modeling studies of the Leeuwin Current off Western and Southern Australia. *Journal of Physical Oceanography*, 28(11), 2199-2221.

Clarke, A.J., Liu, X. (1994). Interannual sea level in the northern and eastern Indian ocean., *Journal of Physical Oceanography*, vol.. vol 24, pp. 1224–1235.

Cresswell, G.R., and Golding, T.J. (1979). Satellite-tracked buoy data report III. Indian Ocean 1977, Tasman Sea July–December 1977. CSIRO Australia Division of Fisheries and Oceanography Rep. 101.

Feng, M., Meyers, G., Pearce, A., and Wijffels, S. (2003). Annual and interannual variations of the Leeuwin Current at 32°S. *Journal of Geophysical Research*, vol. 108, no. C11, p. 3355, doi:10.1029/2002JC001763.

Feng M, Li Y. and Meyers G . (2004). Multidecadal variations of Fremantle sea level: Footprint of climate variability in the tropical Pacific. *Geophysical Research Letters*, vol 31, L16302,doi:10.1029/2004GL019947.

Feng, M., Wifffels, S., Godfrey, S., and Meyers, G . (2005). Do eddies play a role in the momentum balance of the Leeuwin Current? *Journal of Physical Oceanography*, vol. 35, pp. 964–975.

Godfrey, J.S., K.R. Ridgway, K.R. (1985). The large-scale environment of the poleward-flowing Leeuwin Current , Western Australia: Longshore steric height gradients, wind stresses, and geostrophic flow. *Journal of Physical Oceanography*, vol. 15, pp. 481–495.

Godfrey J.S. (1996). The effect of the Indonesian throughflow on ocean circulation and heat exchange with the atmosphere: A review. *Journal of Geophysical Research* , vol. 101, No. C5, pp 12,217-12,237.

Harrison, D.E.,. and Larkin, N.K. (1998). El Niño-Southern Oscillation sea surface temperature and wind anomalies, 1946–1993. *Review of Geophysics*, vol. 36, no. 3, pp. pages 353–-399.

Kiem, A.S., and Franks, S.W. (2001). On the identification of ENSO-induced rainfall and runoff variability: a comparison of methods and indices. *Hydrological Sciences-Journal des Sciences Hydrologiques*, vol. 46, no. 5.

McCreary, J. P., Jr,., S. R. Shetye, S.R.,and P. K. Kundu, P.K. (1986). Thermohaline forcing of eastern boundary currents: with application to the circulation off the west coast Australia. *Journal of Marine Research*, vol.*. Mar. Res.,* 44**,** pp. 71–92.

Mantua, N.J., Hare, S.R., Zhang, Y., Wallace, J.M., and Francis, R.C. (1997). A Pacific interdecadal climate oscillation with impacts on salmon production. Bulletin of the American Meteorological Society, vol. 78, pp. 1069–-1079.

Meyers G. (1996). Variation of Indonesian Throughflow and the El Niño-Southern Oscillation. *Journal of Geophysical Research*, vol. 101, no. C5, pp. 12,255–-12,263.

Meyers, G., Bailey, R.J., Worby, A.P. (1995). Geostrophic transport of Indonesian Throughflow. *Deep-Sea Research I,* vol. 42, no. 7.

Pearce, A.F., and Griffiths, R.W. (1991). The mesoscale structure of the Leeuwin Current: a comparison of laboratory model and satellite images. *Journal of Geophysical Research*, vol. 96, pp. 16730–-16757.

Pearce, A., Pattiarachi, C. (1999). The Capes Current: a summer countercurrent flowing past Cape Leeuwin and Cape Naturaliste, Western Australia. *Continental Shelf Research*, vol. 19, no. 3, pp. 401–420.

Smith, R.L., Huyer, A., Godfrey, J.S., and Church, J.A. (1991). The Leeuwin Current off Western Australia, 1986–1987. *Journal of Physical Oceanography*, vol. 21, pp. 323–345.

Thompson, R.O.R.Y. (1984). Observations of the Leeuwin Current off Western Australia. *Journal of Physical Oceanography*, vol. 21, pp. 323–-345.

Trenberth, K.E., Caron, J.M, Stepaniak, D.P., Worley, S. (2002). Evolution of El Niño-Southern Oscillation and global atmospheric surface temperatures. *Journal of Geophysical Research*, vol. 107, no. D8, 10.1029/2000JD000298.

Van Loon, H. (1972a). Pressure in the Southern Hemisphere. *Meteorological Monographs*, vol. 13, no. 35, *Amer. Meteor. Soc*., pp. 59–-86.

Van Loon, H. (1972b). Temperature in the Southern Hemisphere. *Meteorological Monographs*, vol. No. 13, no. 35, *Amer. Meteor. Soc*., pp. 25-58.

Wijffels, S., and G. A. Meyers, G.A. (2004). An Intersection of Oceanic Wave guides: Variability in the Indonesian Throughflow region. *J. Physical Oceanography*, vol. 34, pp. 1232–-1253.

Zhang, Y., J.M. Wallace, J.M., and D.S. Battisti, D.S. (1997). ENSO-like Interdecadal Variability: 1900–93. *Journal of Climate*, vol. 10, pp. 1004–1020.

Conference attendance and presentations

M. Feng. Latitudinal response of the Leeuwin Current to inter-annual forcing using SODA re-analysis data, poster. session, 2006 Ocean Sciences Meeting., 20–24 February 2006, Honolulu, Hawaii, USA.

Publications and/or outcomes to date

Berthot, A., Pattiaratchi, C.B., Feng, M., Li, Y., and Meyers, G. (2006). Latitudinal response of the Leeuwin Current to inter-annual forcing using SODA re-analysis data. To be submitted to Journal of Geophysical Research.

3.3.4 Ecological Interactions in Coastal Marine Ecosystems: Trophodynamics

Principal Investigators / Institutions

Dr Glenn Hyndes	Senior Lecturer, School of Natural Sciences, Edith Cowan University, 100 Joondalup Drive, Joondalup WA 6027 Phone: 6304 5798 Fax: 6304 5509 Email: g.hyndes@ecu.edu.au
Dr Christine Hanson	Postdoctoral Research Fellow, School of Natural Sciences, Edith Cowan University, 100 Joondalup Drive, Joondalup WA 6027 Phone: 6304 5880 Fax: 6304 5509 Email: c.hanson@ecu.edu.au
Emily Gates	Honours Student, School of Natural Sciences, Edith Cowan University, 100 Joondalup Drive, Joondalup WA 6027 Phone: 6304 2298 Fax: 6304 5509

Co-Investigators / Institutions

Dr Mat Vanderklift	Research Scientist, CSIRO Marine and Atmospheric Research, Underwood Ave, Floreat WA 6014 Phone: 9333 6536 Fax: 9333 6555 Email: mat.vanderklift@csiro.au
Dr Russ Babcock	Senior Research Scientist, CSIRO Marine and Atmospheric Research, Underwood Ave, Floreat WA 6014 Phone: 9333 6535 Fax: 9333 6555 Email: russ.babcock@csiro.au

Note: This project commenced in 2005, and this report presents preliminary findings only.

Executive Summary

Two major seasonal field studies (Autumn and Spring 2005) have been completed for the Trophodynamics project, and work is well underway towards interpreting the food web dynamics of the Jurien Bay Marine Park region. Over 500 samples have been analysed for carbon and nitrogen isotopic signatures, with an initial focus on elucidating the grazing pathway (which includes seagrass, seagrass leaf epiphytes, brown algae, red algae, gastropods and sea urchins) for Autumn 2005.

We found a distinct isotopic separation of the seagrass/epiphyte group from the red and brown algae, although some overlap in $\delta^{13}C$ signatures between the brown and red algae makes